Relative Earthquake Hazard Maps
for selected coastal communities in Oregon

Astoria-Warrenton

Brookings

Coquille

Florence-Dunes City

Lincoln City

Newport

Reedsport-Winchester Bay

Seaside-Gearhart-Cannon Beach

Tillamook

A 1991 earthquake in Costa Rica (M 7.5) damaged rail lines and containers but left the pier and crane undamaged. (Photo from Earthquake Engineering Research Institute)

Oregon Department of Geology and Mineral Industries
Interpretive Map Series
IMS-10
Ian P. Madin and Zhenming Wang
1999

STATE OF OREGON
DEPARTMENT OF GEOLOGY AND MINERAL INDUSTRIES
Suite 965, 800 NE Oregon St., #28
Portland, Oregon 97232

Interpretive Map Series
IMS–10

Relative Earthquake Hazard Maps for Selected Urban Areas in Western Oregon

Astoria-Warrenton, Brookings, Coquille, Florence-Dunes City, Lincoln City, Newport, Reedsport-Winchester Bay, Seaside-Gearhart-Cannon Beach, Tillamook

By
Ian P. Madin and Zhenming Wang
Oregon Department of Geology and Mineral Industries

1999

Funded by the State of Oregon
and the U.S. Geological Survey (USGS), Department of the Interior,
under USGS award number 1434–97–GR–03118

CONTENTS

NOTICE

The results and conclusions of this report are necessarily based on limited geologic and geophysical data, as described in this report. At any given site in any map area, site-specific data could give results that differ from those shown on this map. **THIS REPORT CANNOT REPLACE SITE-SPECIFIC INVESTIGATIONS**. Some appropriate uses are discussed in the report. The hazards of an individual site should be assessed through geotechnical or engineering geology investigation by qualified practitioners.

IMS–10
Relative Earthquake Hazard Maps for Selected Urban Areas in Western Oregon

Astoria-Warrenton, Brookings, Coquille, Florence-Dunes City, Lincoln City, Newport, Reedsport-Winchester Bay, Seaside-Gearhart-Cannon Beach, Tillamook

By Ian P. Madin and Zhenming Wang, Oregon Department of Geology and Mineral Industries

This is one of four companion publications presenting earthquake hazard maps for small to intermediate-sized communities in western Oregon. Each publication includes a geographic grouping of urban areas.

INTRODUCTION

Since the late 1980s, the understanding of earthquake hazards in the Pacific Northwest has significantly increased. It is now known that Oregon may experience damaging earthquakes much larger than any that have been recorded in the past (Atwater, 1987; Heaton and Hartzell, 1987; Weaver and Shedlock, 1989; Yelin and others, 1994). Planning the response to earthquake disasters and strengthening homes, buildings, and lifelines for power, water, communication, and transportation can greatly reduce the impact of an earthquake. These measures should be based on the best possible forecast of the amount and distribution of future earthquake damage. Earthquake hazard maps such as those in this publication provide a basis for such a forecast.

The amount of damage sustained by a building during a strong earthquake is difficult to predict and depends on the size, type, and location of the earthquake, the characteristics of the soils at the building site, and the characteristics of the building itself. At present, it is not possible to accurately forecast the location or size of future earthquakes. It is possible, however, to predict the behavior of the soil[1] at any particular site. In fact, in many major earthquakes around the world, a large amount of the damage has been due to the behavior of the soil.

The maps in this report identify those areas in selected Oregon communities that will be at higher risk, relative to other areas, during a damaging earthquake. The analysis is based on the behavior of the soils and does not depict the absolute earthquake hazard at any particular site. **It is quite possible that, for any given earthquake, damage in even the highest hazard areas will be light. On the other hand, during an earthquake that is stronger or much closer than our design parameters, even the lowest hazard categories could experience severe damage.**

This report includes a nontechnical description of how the maps were made and how they might be used. More technical information on the mapmaking methods is contained in the Appendix.

The printed report includes paper-copy *Relative Earthquake Hazard Maps* for each urban area, overlaid on U.S. Geological Survey topographic base maps at the scale of 1:24,000. In addition, for each area, three individual hazard component maps are included as digital data files on CD-ROM. The digital data are in two formats: (1) high-resolution -.JPG files (bitmap images) that can be viewed with many image viewers or word processors and (2) MapInfo® and ArcView® GIS vector files.

These maps were produced by the Oregon Department of Geology and Mineral Industries and were funded by the State of Oregon and the U.S. Geological Survey (USGS), Department of the Interior, under USGS award #1434-97-GR-03118. The views and conclusions contained in this document are those of the authors and should not be interpreted as necessarily representing the official policies, either expressed or implied, of the U.S. Government.

[1] In this report, "soil" means the relatively loose and soft geologic material that typically overlies solid bedrock in western Oregon.

EARTHQUAKE HAZARD

Earthquakes from three different sources threaten communities in western Oregon (Figure 1). These sources are crustal, intraplate, and subduction-zone earthquakes. The most common are crustal earthquakes, which typically occur in the North American plate above the subduction zone at relatively shallow depths of 6–12 mi (10–20 km) below the surface. The March 1993 earthquake at Scotts Mills (magnitude [M] 5.6) (Madin and others, 1993) and the September 1993 Klamath Falls main shocks (M 5.9 and M 6.0) (Wiley and others, 1993) were such crustal earthquakes.

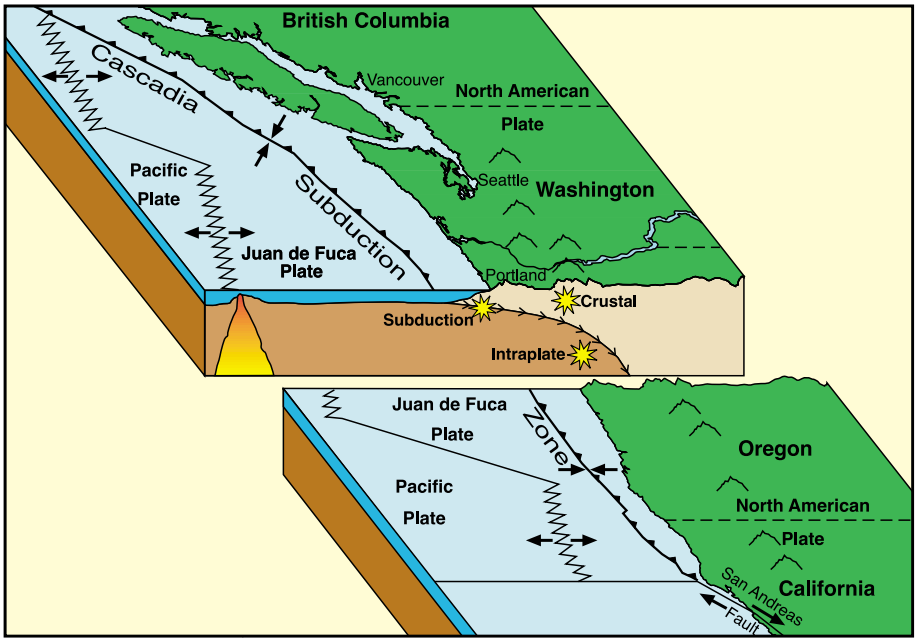

Figure 1. Plate-tectonic map of the Pacific Northwest. Oregon is cut in half to show where earthquakes originate below the surface (asterisks).

Deeper intraplate earthquakes occur within the remains of the ocean floor (the Juan de Fuca plate) that has been subducted beneath North America. Intraplate earthquakes caused damage in the Puget Sound region in 1949 and again in 1965. This type of earthquake could occur beneath much of western Oregon at depths of 25–37 mi (40–60 km).

Great subduction-zone earthquakes occur around the world where the plates that make up the surface of the Earth collide. When the plates collide, one plate slides (subducts) beneath the other, where it is reabsorbed into the mantle of the planet. The dipping interface between the two plates is the site of some of the most powerful earthquakes ever recorded, often having magnitudes of M 8 to M 9 on the moment magnitude scale. The 1960 Chilean (M 9.5) and the 1964 Great Alaska (M 9.2) earthquakes were subduction-zone earthquakes (Kanamori, 1977). The Cascadia subduction zone, which lies off the Oregon and Washington coasts, has been recognized for many years. No earthquakes have occurred on the Cascadia subduction zone during our short 200-year historical record. However, in the past several years, a variety of studies have found widespread evidence that very large earthquakes have occurred repeatedly in the past, most recently about 300 years ago, in January 1700 (Atwater, 1987; Yamaguchi and others, 1997). The best available evidence indicates that these earthquakes occur, on average, every 500 to 540 years, with an interval between individual events that ranges from 100–300 years to about 1,000 years (Atwater and Hemphill-Haley, 1997). We have every reason to believe that they will continue to occur in the future.

Together, these three types of earthquakes could cause strong shaking through most of western Oregon. Maps are available that forecast the likely strength of shaking for all of Oregon (Geomatrix Consultants, 1995; Frankel and others, 1996; Madin and Mabey, 1996). However, these maps show the expected strength of shaking at a firm site on bedrock and do not include the significant influence of soil on the strength of shaking. They forecast a uniform level of shaking and damage in most communities, and as such they do not provide a useful tool for planning earthquake hazard mitigation measures.

EARTHQUAKE EFFECTS

Damaging earthquakes will occur in the cities and towns of western Oregon. This fact was demonstrated by the Scotts Mills earthquake (M 5.6) in 1993 (Madin

and others, 1993). Although we cannot predict when the next damaging earthquake will strike, where it will occur, or how large it will be, we can evaluate the influence of site geology on potential earthquake damage. This evaluation can occur reliably even though the exact sources of earthquake shaking are uncertain.

The most severe damage done by an earthquake is commonly localized. One or more of the following phenomena generally will cause the damage in these areas:

1. Amplification of ground shaking by a "soft" soil column.

2. Liquefaction of water-saturated sand, silt, or gravel creating areas of "quicksand."

3. Landslides triggered by shaking, even on relatively gentle slopes.

These effects can be evaluated before the earthquake occurs, if data are available on the thickness and nature of the geologic materials and soils at the site (Bolt, 1993). Knowing the exact nature and magnitude of these effects is useful to technical professionals, and such data (in digital format) are included in this publication. For others, what is more significant is that these effects increase the damage caused by an earthquake and localize the most severe damage.

HAZARD MAP METHODOLOGY

Selection of map areas

Urban areas were mapped if they had a population greater than 4,000, were in Uniform Building Code (UBC) Seismic Zone 3 or 4, and were not likely to be the subject of a more detailed future hazard mapping program. The goal of this project was to provide an inexpensive general hazard assessment for small communities that could not afford their own mapping program but were not large enough to justify a major state-funded mapping effort. Such major, full-scale projects have been undertaken for the Portland, Salem, Eugene-Springfield, and Klamath Falls urban areas; they typically take several years and cost several hundred thousand dollars. In contrast, this project involved about two weeks of work and a few thousand dollars for each urban area mapped.

For each urban area selected, the hazard map area (inside the thick black line) was defined by the urban growth boundary plus a 3,300-ft (1-km)-wide buffer.

Geologic model

The most important element of any earthquake hazard evaluation is the development of a three-dimensional geologic model. For analysis of the amplification and liquefaction hazards, the most important feature is the thickness of the loose sand, silt, and gravel deposits that usually overlie firm bedrock. For an analysis of the landslide hazard, the steepness of the slopes and presence of existing landslides is important. For each urban area, the geologic model was developed as follows:

The best available geologic mapping was used to determine what geologic materials were present and where they occurred. Air photos were used to help make these decisions where the mapping was poor or of low resolution. All data were plotted digitally on USGS Digital Raster Graphics (DRG) maps (the digital equivalent of USGS 1:24,000-scale topographic maps).

Drillers' logs of water wells were examined to determine the geology beneath the surface and map the thickness of the loose surficial deposits and the depth to firm bedrock. Water wells were located according to the location information provided on the logs, which often is accurate only to within about 1,000 ft. Field location of the individual logs would have been prohibitively expensive.

The water well data were combined with the surface data to produce a three-dimensional geologic model, describing the thickness of the various geologic materials in the top 100 ft (30 m) throughout each urban area. For this procedure, MapInfo® and Vertical Mapper® Geographic Information System (GIS) software programs were used. The models take the form of a grid of thickness values spaced every 165 ft (50 m).

The resultant models were reviewed by geologists knowledgeable about each area, who judged whether the models were reasonable and consistent with the data.

Existing landslides were mapped where depicted on existing geologic maps or where air photos showed clear signs of landslide topography.

Slope data were derived from USGS Digital Elevations Models (DEMs) with elevation data every 100 ft (30 m). They were then used in MapInfo® and Vertical Mapper® to map the steepness of slopes.

The details of the local geology and data sources for each urban area are described in the "Urban Area Summaries" section of this report.

Hazard analysis

Ground shaking amplification

The soils and soft sedimentary rocks near the surface can modify bedrock ground shaking caused by an earthquake. This modification can increase (or decrease) the strength of shaking or change the frequency of the shaking. The nature of the modifications is determined by the thickness of the geologic materials and their physical properties, such as stiffness.

This amplification study used a method first developed for the National Earthquake Hazard Reduction Program (NEHRP) and published by the Federal Emergency Management Agency (FEMA, 1995). This method was adopted in the 1997 version of the Uniform Building Code (ICBO [International Conference of Building Officials], 1997) and will henceforth be referred to as the UBC-97 methodology. The UBC-97 methodology defines six soil categories that are based on average shear-wave velocity in the upper 100 ft (30 m) of the soil column. The shear-wave velocity is the speed with which a particular type of ground vibration travels through a material, and can be measured directly by several techniques. The six soil categories are Hard Rock (A), Rock (B), Very Dense Soil and Soft Rock (C), Stiff Soil (D), Soft Soil (E), and Special Soils (F). Category F soils are very soft soils requiring site-specific evaluation and are not mapped in this study, because limited funding precluded any site visits.

For the amplification hazard component maps, we collected shear-wave velocity data (see Appendix for data and methods) at one or more sites in each urban area and used our geologic model to calculate the average shear-wave velocity of each 165-ft (50-m) grid cell in the model. We then assigned a soil category, using the relationships in Table 1.

According to the UBC-97 methodology, none of the urban areas in this study had Type A soils. UBC-97 soil category maps for each urban area are presented in the accompanying digital map set.

Table 1. *UBC-97 soil profile types. From ICBO, 1997*

Soil category	Description	Average shear-wave velocity meters/second	Amplification factor (Cv)
S_A	Hard rock	Vs > 1,500	0.8
S_B	Rock	760 < Vs < 1,500	1
S_C	Very dense soil and soft rock	360 < Vs < 760	1.5
S_D	Stiff soil	180 < Vs < 360	1.8
S_E	Soil	Vs < 180	2.8
S_F	Soil requiring site-specific evaluation		

Liquefaction

Liquefaction is a phenomenon in which shaking of a saturated soil causes its material properties to change so that it behaves as a liquid. In qualitative terms, the cause of liquefaction was described very well by Seed and Idriss (1982): "If a saturated sand is subjected to ground vibrations, it tends to compact and decrease in volume; if drainage is unable to occur, the tendency to decrease in volume results in an increase in pore water pressure, and if the pore water pressure builds up to the point at which it is equal to the overburden pressure, the effective stress becomes zero, the sand loses its strength completely, and it develops a liquefied state."

Soils that liquefy tend to be young, loose, granular soils that are saturated with water (National Research Council, 1985). Unsaturated soils will not liquefy, but they may settle. If an earthquake induces liquefaction, several things can happen: The liquefied layer and everything lying on top of it may move downslope. Alternatively, it may oscillate with displacements large enough to rupture pipelines, move bridge abutments, or rupture building foundations. Light objects, such as underground storage tanks, can float toward the surface, and heavy objects, such as buildings, can sink. Typical displacements can range from centimeters to meters. Thus, if the soil at a site liquefies, the damage resulting from an earthquake can be dramatically increased over what shaking alone might have caused.

The liquefaction hazard analysis is based on the age and grain size of the geologic unit, the thickness of the unit, and the shear-wave velocity. Use of the shear-wave velocity to characterize the liquefaction potential follows Andrus and Stokoe (1997). Liquefaction hazard categories were assigned according to Table 2. In all communities we assumed that the susceptible units

Table 2. *Liquefaction hazard categories*

Shearwave velocity (meters/second)	Geologic units (see Appendix) Qs, Qe, Qaf	Qmf, Qmf1, Qmf2, QPe, Qmt	Qac,QTac, QTaf, Qmc	Tbs, Tbv, Grus, KJg, KJm
Greater than 200	Moderate	Low	None	None
100 to 200	High	Moderate	Low	None
Less than 100	High	High	Moderate	None

Thickness adjustment

Unit thickness (m)	Adjustment
Less than 0.5	Down 2 categories
0.5 to 3.0	Down 1 category
Greater than 3.0	No change

were saturated. This is reasonable and conservative, since most of the susceptible units are either alluvial deposits in floodplains, coastal deposits, or silt deposits in areas of low relief and high rainfall in the Willamette Valley.

Earthquake-induced landslides

The hazard due to earthquake-induced landsliding was assessed with slope data derived from USGS DEMs with 100-ft (30-m) data spacing and from mapping of existing slides, either from air photo interpretation or published geologic maps. The analysis was based on methods used by Wang, Y., and others (1998) and Wang, Z., and others (1999) but was greatly simplified because no field data were available. Earthquake-induced landslide hazard categories were assigned according to Table 3.

Table 3. *Earthquake-induced landslide hazard zones*

Slope angle (degrees)	Hazard category
Less than 5	Low
5 to 25	Moderate
Greater than 25	High
Existing landslides	High

RELATIVE EARTHQUAKE HAZARD MAPS

The *Relative Earthquake Hazard Map* is a composite hazard map depicting the relative hazard at any site due to the combination of the effects mentioned above. It delineates those areas that are most likely to experience the most severe effects during a damaging earthquake. Areas of highest risk are those with high ground amplification, high likelihood of liquefaction, existing landslides, or slopes steeper than 25°. Planners, lenders, insurers, and emergency responders can use these simple composite hazard maps for general hazard mitigation or response planning.

It is very important to note that the relative hazard map predicts the tendency of a site to have greater or lesser damage than other sites in the area. These zones, however, should not be used as the sole basis for any type of restrictive or exclusionary development policy.

The *Relative Earthquake Hazard Maps* were created to show which areas will have the greatest tendency to experience damage due to any combination of the three hazards described above. For the purpose of creating the final relative hazard map for each urban area, the zones in each of the three component maps were assigned numerical values according to Table 4.

For every point (in a 165-ft [30-m] grid spacing) on the map, the zone rating for each individual hazard type was squared, and the resulting numbers were added together. Then the square root of this sum was taken and rounded to the nearest whole number. A result of 4 or more was assigned to Zone A, 3 to Zone B, 2 to Zone C, and 1 to Zone D.

While the production of the individual hazard maps is different from previous DOGAMI relative earthquake studies (Wang and Priest, 1995; Wang and Leonard, 1996; Mabey and others, 1997), the method of production of the final relative hazard map is very similar. Thus, these relative hazard maps are directly comparable to DOGAMI studies in Eugene-Springfield, Portland, Salem, and Siletz Bay.

Table 4. *Hazard zone values assigned to the individual relative earthquake hazard map zones*

Relative hazard zone value	Amplification hazard (UBC-97 category S-)	Liquefaction hazard	Landslide hazard
0	B	None	None
1	C	Low	—
1.5	—	—	Moderate
2	D	Moderate	—
3	E	High	High

The GIS techniques used to develop these maps involved several changes between vector data and raster data, with a data grid cell size of 165 ft (50 m) for the raster data. As a result, the relative hazard maps often had numerous zones that were very small, and probably not significant. The final maps were hand-edited to remove all hazard zones that covered less than 1 acre.

USE OF RELATIVE EARTHQUAKE HAZARD MAPS

The *Relative Earthquake Hazard Maps* delineate those areas most likely to experience damage in a given earthquake. This information can be used to develop a variety of hazard mitigation strategies. The information should, however, be carefully considered and understood, so that inappropriate use can be avoided.

Emergency response and hazard mitigation

One of the key uses of these maps is to develop emergency response plans. The areas indicated as having a higher hazard would be the areas where the greatest and most abundant damage will tend to occur. Planning for disaster response will be enhanced by the use of these maps to identify which resources and transportation routes are likely to be damaged.

Land use planning and seismic retrofit

Efforts and funds for both urban renewal and strengthening or replacing older and weaker buildings can be focused on the areas where the effects of earthquakes will be the greatest. The location of future urban expansion or intensified development should also consider earthquake hazards.

Requirements placed on development could be based on the hazard zone in which the development is located. For example, the type of site-specific earthquake hazard investigation that is required could be based on the hazard.

Lifelines

Lifelines include road and access systems including railroads, airports, and runways, bridges, and over- and underpasses, as well as utilities and distribution systems. The *Relative Earthquake Hazard Map* and its component single-hazard maps are especially useful for expected-damage estimation and mitigation for lifelines. Lifelines are usually distributed widely and often require regional as opposed to site-specific hazard assessments. The hazard maps presented here allow quantitative estimates of the hazard throughout a lifeline system. This information can be used for assessing vulnerability as well as deciding on priorities and approaches for mitigation.

Engineering

The hazard zones shown on the *Relative Earthquake Hazard Maps* cannot serve as a substitute for site-specific evaluations based on subsurface information gathered at a site. The calculated values of the individual component maps used to make the *Relative Hazard Maps* may, however, be used to good purpose in the absence of such site-specific information, for instance, at the feasibility-study or preliminary-design stage. In most cases, the quantitative values calculated for these maps would be superior to a qualitative estimate based solely on lithology or non-site-specific information. Any significant deviation of observed site geology from the geologic model used in the analyses indicates the need for additional analyses at the site.

Relative hazard

It is important to recognize the limitations of a *Relative Earthquake Hazard Map*, which in no way includes information with regard to the probability of damage to occur. Rather, it shows that when shaking occurs, the damage is more likely to occur, or be more severe, in the higher hazard areas. The exact probability of such shaking to occur is yet to be determined.

Neither should the higher hazard areas be viewed as unsafe. Except for landslides, the earthquake effects that are factored into the *Relative Earthquake Hazard Map* are not life threatening in and of themselves. What is life threatening is the way that structures such as buildings and bridges respond to these effects.

The map depicts trends and tendencies. In all cases, the actual threat at a given location can be assessed only by some degree of site-specific assessment. This is similar to being able to say demographically that a zip code zone contains an economic middle class, but within that zone there easily could be individuals or neighborhoods significantly richer or poorer.

Because the maps exist as “layers” of digital GIS data, they can easily be combined with earthquake source information to produce earthquake damage scenarios. They can also be combined with probabilistic or scenario bedrock ground shaking maps to provide an assessment of the absolute level of hazard and an estimate of how often that level will occur. Finally, the maps can also be easily used in conjunction with GIS data for land use or emergency management planning.

This study does not address the hazard of tsunamis that exists in areas close to the Oregon coast and is also earthquake induced. The Oregon Department of Geology and Mineral Industries has published separate tsunami hazard maps on this subject (Priest, 1995; Priest and Baptista, 1995).

URBAN AREA SUMMARIES

ASTORIA-WARRENTON URBAN AREA

The Astoria-Warrenton geologic model was developed using airphoto interpretation, surface geologic data from Schlicker and others (1972) and subsurface data from 21 approximately-located water wells.

The geology of this area was difficult to model because of the very sparse subsurface data set available. The model was largely derived by assuming that the area has been drowned in Quaternary sediment deposited by the Columbia River and its local tributaries as sea level has risen, and that the bedrock (Tbs) topography beneath the Quaternary sediments looks similar to that above. Shear wave velocity sites were used to fill in data gaps for the thickness of the estuarine sediments. The model consists of a body of Quaternary sand (Qs) and a body of Quaternary estuarine clay and silt (Qe). Units are described in Appendix 1.

Existing landslides are common in the area, particularly in urban Astoria.

Shear wave velocities are assigned to the units as follows:

Qe Three direct measurements, ranging from 70 to 95 m / sec, average 82 m / sec.

Qs Five direct measurements, ranging from 133 to 210 m / sec, average 173 m / sec.

Tbs One direct measurement, 523 m / sec.

Amplification hazard is high on the Clatsop plain and floodplains of the Columbia and tributaries due to thick deposits of Qs and Qe. Amplification hazard is low in the adjacent hills, which are bedrock.

Liquefaction hazard is high on the Clatsop plain and floodplains of the Columbia and tributaries due to thick deposits of Qs and Qe. Liquefaction hazard is nil in the adjacent hills, which are bedrock.

Earthquake-induced landslide hazard is low on the Clatsop plain and floodplains of the Columbia and tributaries. Landslide hazard is generally moderate in the adjacent hills, except for large areas of existing landslide, which have high hazard.

Relative hazard is generally Zone A for the Clatsop plain and floodplains of the Columbia and its tributaries due to high amplification and liquefaction hazard. The adjacent hills are mostly in Zone C and B, due to high to moderate landslide and low amplification hazards.

BROOKINGS URBAN AREA

The geologic model for the Brookings area was developed using surface geologic data at 1:62,500 from Beaulieu and Hughes (1976), unpublished 1:24,000-scale mapping of marine terraces by Dr. Harvey Kelsey of Humboldt State University, and subsurface data from 64 approximately located water and geotechnical wells. The geology consists of Quaternary marine terrace sand, silt, and clay (Qmt) deposited over Jurassic melange bedrock (KJm). Quaternary sand and gravel alluvium (Qac) fills the channel of the Chetco River. Units are described in Appendix 1.

The model consists of a body of marine terrace sediments over bedrock and a body of Quaternary alluvium over terrace sediments.

Shear wave velocities are assigned to the units as follows:

Qac No direct measurements, Qac at other similar sites averages 223 m/sec.

Qmt One direct measurement, 481 m/sec.

KJm One direct measurement, 1,172 m/sec.

Amplification is nil in most of the area, with the exception of the floodplain of the Chetco River, where it is high.

Liquefaction is probably a minimal hazard in most of the area, because the terrace sediments are high-velocity and fairly weathered (drillers report many hard or cemented horizons). Liquefaction hazard is restricted to the Quaternary alluvium along the Chetco River.

Although slopes are steep, there are no obvious prehistoric landslides and no mapped slides, possibly because the bedrock is very competent. Earthquake-induced landslide hazard is restricted to the steepest slopes.

The majority of the area is in relative hazard Zone D, reflecting low or no hazard in most categories. The exceptions are some of the steepest slopes and the alluvium along the Chetco River.

COQUILLE URBAN AREA

The geologic model for the Coquille area was developed using 1:62,500-scale surface geologic data from Beaulieu and Hughes (1975) and subsurface geologic data from 24 approximately located water wells. The geology consists of Pleistocene and Holocene alluvial silt and clay (Qaf) deposited on Eocene sedimentary bedrock (Tbs). The model consists of a single body of Qaf over bedrock. Units are described in Appendix 1.

Shear wave velocities were assigned as follows:

Qaf Two direct measurements, 151 and 191 m/sec, average 171 m/sec.

Tbs Two direct measurements, 385 and 589 m/sec, average 487 m/sec.

Amplification is low in the bedrock slopes around Coquille and moderate to high on the flats adjacent to the Coquille River and its major tributaries.

Liquefaction hazard is moderate to high adjacent to the Coquille River and its major tributaries.

Earthquake-induced landslide hazard is generally low to moderate, with a few areas of high hazard on old landslides or in a few very steep areas in the hills surrounding the urban area.

Most of the flat areas along the Coquille River and its tributaries are in relative hazard Zones A and B, reflecting high amplification and liquefaction hazards. The surrounding hills are generally in Zone C, with areas of Zone B associated with steep slopes and existing landslides.

FLORENCE-DUNES CITY URBAN AREA

The Florence-Dunes City geologic model was developed using surface geology from Schlicker and others (1974) and subsurface data from 69 approximately located water wells. The geology of the area consists of Holocene beach dune sands (Qs) on top of sedimentary bedrock of the Eocene Tyee formation (Tbs). The geologic model consists of a body of Qs over bedrock. Units are described in Appendix 1.

Shear wave velocities are assigned as follows:

Qs Five direct measurements, ranging from 174 to 371 m/sec, average 263 m/sec.

Tbs One direct measurement, 576 m/sec.

Amplification is low in the bedrock areas of the urban area, and moderate in the flatter areas underlain by Qs.

Liquefaction is likely to be a widespread hazard in Qs, given the abundance of young clean dune sands and a relatively shallow water table.

Earthquake-induced landslide hazard is generally low, with some areas moderate on the steepest slopes.

Most of the coastal plain is in relative hazard Zone A, reflecting a combination of liquefaction and amplification hazards. Inland, the hilly areas are generally Zone C, reflecting moderate slope hazards and low amplification.

LINCOLN CITY URBAN AREA

The Lincoln City geologic model was derived from surface geologic data in Snavely and others (1976), Wang and Priest (1995), and unpublished detailed mapping by Dr. George Priest of DOGAMI. Subsurface geology was mapped using data from 38 approximately located water wells, 4 drill holes or cone penetrometer profiles from Wang and Priest (1995) and two shear wave refraction profiles produced for this study.

The geology consists of Quaternary marine terrace deposits (Qmt) and Quaternary alluvial, estuarine, and beach deposits (Qs) overlying Tertiary marine sedimentary rocks with some basaltic intrusive rocks (Tbs). Units are described in Appendix 1.

The marine terrace sediments consist of one extensive terrace surface and numerous small patches of uplifted and dissected terrace. The alluvial and estuarine deposits consist of sand, silt, and clay filling the ancestral Siletz River valley in what is now Siletz Bay. Available data are not sufficient to map the estuarine clays separately from the alluvial sands, but the clays are apparently fairly rare, as indicated by data from Wang and Priest (1995), and are combined in a single alluvial unit in this study. Similarly, beach deposits could not be readily distinguished from the sand alluvium; but they have similar velocities and so are combined with the alluvium.

Shear wave velocities are assigned as follows:

Qs Five direct measurements, 129 to 282 m/sec, average 214 m/sec.

Qmt Two direct measurements, 185 and 334 m/sec, average 259 m/sec.

Tbs Two direct measurements, 958 and 626 m/sec, average 792 m/sec.

Amplification hazard is nil in the hilly bedrock areas, low on the terraces between the hills and the beach, and moderate in the middle of Siletz Bay where the Qs is very thick.

Liquefaction hazard is nil in the hilly bedrock areas, low on the flat terraces between the hills and the beach, and moderate to high on the flats surrounding Devils Lake and Siletz Bay.

Earthquake-induced landslide hazard is low on the flats around Siletz Bay and Devils Lake and on the flat terraces between the hills and the beach. In the hills, landslide hazard is generally moderate, except for several areas of existing landslides and a few areas of very steep slopes.

The majority of the area is in relative hazard Zone D, with areas up to Zone B around Devils Lake and up to Zone D in Siletz Bay. There are scattered areas up to Zone B in the hills associated with existing landslides.

.

NEWPORT URBAN AREA

The Newport geologic model was developed using unpublished surface geologic data from Dr. George Priest, and data from Ticknor (1993). Subsurface geology was inferred from Ticknor (1993) and from 32 approximately located water wells. The geology consists of marine terrace sediments of late Quaternary age (Qmt) and Holocene sand silt and clay alluvium (Qs) over Tertiary mudstone and basalt bedrock (Tbs). Units are described in Appendix 1.

The alluvium is restricted to Yaquina Bay and the low-elevation bench at South Beach. Existing landslides on the bedrock slopes in the area are common, as are slides along the bluffs above the coastline.

Shear wave velocities are assigned as follows:

Qmt One direct measurement, 448 m/sec.

Qs We took measurements at one site on Qs (site Newp02), but the values (324 and 419 m/sec) were anomalously high. The measurements were made near the north jetty and may have been made over artificial fill. Consequently, we used the average value for Qs and Qe sediments at the Lincoln City, Tillamook, and Astoria-Warrenton sites (148 m/sec, average of 12 values).

Tbs One direct measurement, 613 m/sec.

Amplification hazard is low throughout most of the area, reflecting relatively high-velocity Qmt deposits on the terraces and Tbs in the hills. Amplification hazard is generally high in Yaquina Bay, reflecting thick Qs.

Liquefaction hazard is low on the flat terraces between the hills and the coast, reflecting Qmt deposits. Liquefaction hazard in the bedrock hills is nil. Liquefaction hazard in Yaquina Bay is moderate to high, due to thick Qs deposits.

Earthquake-induced landslide hazard is low on the flat terrace surfaces and in Yaquina Bay, moderate on most of the hills surrounding the area, and high in areas of existing landslides both in the hills and along the coastal bluffs.

Much of the area on the flat terraces is in relative hazard Zone D and most of the hilly areas are in Zone C, reflecting moderate slope hazard. Areas of Zone B are common in the hills and along the coastal bluffs, associated with existing landslides. Yaquina Bay and the surrounding flats are in Zone A, reflecting high liquefaction and amplification hazards.

REEDSPORT-WINCHESTER BAY URBAN AREA

The Reedsport-Winchester Bay geologic model was developed using surface geologic mapping at 1:62,500 (Beaulieu and Hughes, 1975), air photo interpretation, and subsurface data from 30 approximately located water wells. The geology consists of Pleistocene (QPe) and Holocene (Qe) estuarine and alluvial sand, silt, and clay deposited by the Umpqua River over Eocene sedimentary bedrock (Tbs). Units are described in Appendix 1.

The Pleistocene and Holocene deposits occupy the present channel and floodplain of the Umpqua River; at Reedsport, the Pleistocene deposits fill an abandoned meander of the Umpqua River. The geologic model consists of a body of Holocene fine-grained alluvium, a body of Pleistocene sand-and-gravel alluvium, and bedrock.

Shear wave velocities are assigned as follows:

Qe One direct measurement, 89 m/sec.

QPe Two direct measurements, 144 and 142 m/sec, average 143 m/sec.

Tbs One direct measurement, 749 m/sec.

The amplification hazard in the area is generally high, with the exception of areas underlain by bedrock, principally in the hills.

Liquefaction hazard is high in areas of unit Qe, which is predominantly very young and soft silt and sand along the Umpqua River and tributaries. The liquefaction potential is somewhat less in areas underlain by Pe, because it is more consolidated and older. Liquefaction hazard in the hills is nil.

Earthquake-induced landslide hazard is generally moderate in the hills, with significant areas of high hazard due to steep slopes.

Most of the low-lying flats along the Umpqua River and Winchester Creek are in relative hazard Zone A, reflecting high amplification and liquefaction hazards. Most of the surrounding hills are in Zone D, with some areas of higher hazard associated with steep slopes.

SEASIDE-GEARHART-CANNON BEACH URBAN AREA

The Seaside-Gearhart-Cannon Beach geologic model was developed using surface geology from Schlicker and others (1972) and subsurface data from 21 approximately located water wells. The geology of the area consists of Holocene dune and beach sand (Qs) deposits on top of Miocene volcanic and sedimentary bedrock (Tbs). Units are described in Appendix 1.

Large ancient landslides are abundant on the bedrock slopes. Only one well actually penetrated the entire Qs section, so the thickness model is based on the assumption that the bedrock topography beneath the Qs deposits is similar to that exposed above. The geologic model consists of a body of Quaternary dune and beach sands over bedrock. However, Dr. Curt Peterson (oral communication, 1998) indicates that the Quaternary section is quite variable, including buried Holocene gravel bars and beach-sand facies of different densities as well as an underlying layer of denser Pleistocene sands. These varied deposits are reflected in the wide range of measured shear wave velocities, but cannot be mapped ith the data available. Therefore, the Quaternary deposits are treated as a single body, and the measured velocities are averaged.

Shear wave velocities are assigned as follows:

Qs Six direct measurements, 170 to 365 m/sec, average 260 m/sec.

Tbs No direct measurements. Similar rocks to the north at Astoria have velocities of 530 m/sec, and at Tillamook, 610 m/sec. The average used for this site is 570 m/sec.

Amplification hazard throughout most of the area is low, reflecting the bedrock that underlies most of the hilly areas. Amplification hazards on the Seaside-Gearhart coastal plain and the lowland flats at Cannon Beach are moderate, reflecting thick Qs deposits.

Liquefaction hazard is nil in the hills, reflecting bedrock at the surface. Liquefaction hazards on the Seaside-Gearhart coastal plain and the lowland flats at Cannon Beach are high, reflecting thick Qs deposits.

Earthquake-induced landslide hazard is low on the Seaside-Gearhart coastal plain and the lowland flats at Cannon Beach and moderate to high in the surrounding hills. High values are generally associated with existing landslides.

Most of the coastal plain at Seaside-Gearhart, and the lowland flats at Cannon Beach are in relative hazard Zone A, reflecting the combination of moderate amplification hazard and high liquefaction hazard. Most of the surrounding hills are in Zone C, with large areas of Zone B associated with existing landslides.

TILLAMOOK URBAN AREA

The Tillamook geologic model was developed using digital geologic data provided by Dr. Ray Wells of the U.S. Geological Survey, and the subsurface geology was inferred from 48 approximately located water wells.

The geology in Tillamook consists of Holocene estuarine silt, clay, and peat (Qe) overlying Quaternary fluvial sand and gravel (QTac) over Miocene bedrock (Tbs). The bedrock is not exposed anywhere in the target area. The geologic model consists of a body of Qe and a body of QTac. Units are described in Appendix 1.

Shear wave velocities are assigned as follows:

Qe Two direct measurements, 82 and 83 m/sec.

QTac Three direct measurements, 250 to 335 m/sec, average 297 m/sec.

Tbs One direct measurement, 610 m/sec.

Amplification hazard is high in much of the area, due to thick deposits of Qe. There is a large area of moderate amplification hazard at the east end of the area, where Qe is relatively thin. Small areas of low hazard at the east and northwest edges of the area are associated with bedrock exposed in the hills.

Liquefaction hazard is generally high in the area, with an area of moderate hazard in the east, where the Qe is thin, and small amounts of low to nil hazard in the hills.

Earthquake-induced landslide hazard is low throughout the area, reflecting generally low slopes.

Most of the area is in relative hazard Zone A, due to the combination of liquefaction and amplification hazards associated with Qe. The hazard is less in the east, with moderate sized areas of Zone B, C, and D located in the hills and in areas of thin Qe.

ACKNOWLEDGMENTS

Geological models were reviewed by Marshall Gannett and Jim O'Connor of the USGS Water Resources Division, Ken Lite of the Oregon Water Resources Division, Dr. Ray Wells of the US Geological Survey, Dr. Curt Peterson of Portland State University, Dr. Jad D'Allura of Southern Oregon University, Dr. John Beaulieu, Gerald Black and Dr. George Priest of the Oregon Department of Geology and Mineral Industries. The reports were reviewed by Gerald Black and Mei Mei Wang. Marshall Gannett and Jim O'Connor provided unpublished digital geologic data which were helpful in building the geologic models. Dr. Marvin Beeson provided unpublished geologic mapping. We are very grateful to all of these individuals for their generous assistance.

BIBLIOGRAPHY

Andrus, R.D., and Stokoe, K.H., 1997, Liquefaction resistance based on shear-wave velocity (9/18/97 version), *in* Youd, T.L., and Idriss, I.M., eds., Proceedings of the NCEER Workshop on Evaluation of Liquefaction Resistance of Soils, Jan. 4–5, Salt Lake City, Utah: Buffalo, N.Y., National Center for Earthquake Engineering Research Technical Report NCEER-97-0022, p. 89–128.

Atwater, B.F., 1987, Evidence for great Holocene earthquakes along the outer coast of Washington State: Science, v. 236, p. 942–944.

Atwater, B.F., and Hemphill-Haley, 1997, Recurrence intervals for great earthquakes of the past 3,500 years at northeastern Willapa Bay, Washington: U.S. Geological Survey Professional Paper 1576, 108 p.

Baldwin, E.M., 1964, Geology of the Dallas and Valsetz quadrangles, rev. ed.: Oregon Department of Geology and Mineral Industries Bulletin 35, 56 p., 1 map 1:62,500.

Beaulieu, J.D., 1977, Geologic hazards of parts of northern Hood River, Wasco, and Sherman Counties, Oregon: Oregon Department of Geology and Mineral Industries Bulletin 91, 95 p., 10 maps.

Beaulieu, J.D., and Hughes, P.W., 1975, Environmental geology of western Coos and Douglas Counties, Oregon: Oregon Department of Geology and Mineral Industries Bulletin 87, 148 p., 16 maps.

———1976, Land use geology of western Curry County, Oregon: Oregon Department of Geology and Mineral Industries Bulletin 90, 148 p., 12 maps.

Bela, J.L, 1981, Geology of the Rickreall, Salem West, Monmouth, and Sidney 7½' quadrangles, Marion, Polk, and Linn Counties, Oregon: Oregon Department of Geology and Mineral Industries Geological Map Series GMS–18, 2 pls., 1:24,000.

Bolt, B.A., 1993, Earthquakes: New York, W.H. Freeman and Co., 331 p.

Bretz, J.H., Smith, H.T.U., and Neff, G.E., 1956, Channeled Scabland of Washington: New data and interpretations: Geological Society of America Bulletin, v. 67, no. 8, p. 957–1049.

Brownfield, M.E., 1982, Geologic map of the Sheridan quadrangle, Polk and Yamhill Counties, Oregon: Oregon Department of Geology and Mineral Industries Geological Map Series GMS–23, 1:24,000.

Brownfield, M.E., and Schlicker, H.G., 1981, Preliminary geologic map of the McMinnville and Dayton quadrangles, Oregon: Oregon Department of Geology and Mineral Industries Open-File Report O–81–6, 1:24,000.

FEMA (Federal Emergency Management Agency), 1995, NEHRP recommended provisions for seismic regulations for new buildings, 1994 edition, Part 1: Provisions: Washington, D.C., Building Seismic Safety Council, FEMA Publication 222A / May 1995, 290 p.

Frankel, A., Mueller, C., Barnhard, T., Perkins, D., Leyendecker, E.V., Dickman, N., Hanson, S., and Hopper, M., 1996, National seismic hazard maps, June 1996 documentation: U.S. Geological Survey Open-File Report 96–532, 110 p.

Gannett, M.W., and Caldwell, R.R., 1998, Geologic framework of the Willamette Lowland aquifer system: U. S. Geological Survey Professional Paper1424–A, 32 p., 8 pls.

Geomatrix Consultants, Inc., 1995, Seismic design mapping, State of Oregon: Final Report to Oregon Department of Transportation, Project no. 2442, var. pag.

Heaton, T.H., and Hartzell, S.H., 1987, Earthquake hazards on the Cascadia subduction zone: Science, v. 236, no. 4798, p. 162–168.

Hunter, J.A., Pullan, S.E., Burns, R.A., and Good, R.L., 1984, Shallow seismic reflection mapping of the overburden-bedrock interface with an engineering seismograph——Some simple techniques: Geophysics, v. 49, p. 1381–1385.

ICBO (International Conference of Building Officials), 1997, 1997 Uniform building code, v. 2, Structural engineering design provisions: Whittier, Calif., International Conference of Building Officials, 492 p.

Kanamori, H., 1977, The energy release in great earthquakes: Journal of Geophysical Research, v. 82, p. 2981–2987.

Mabey, M.A., Black, G.L., Madin, I.P., Meier, D.B., Youd, T. L., Jones, C.F., and Rice, J.B., 1997, Relative earthquake hazard map of the Portland metro region, Clackamas, Multnomah, and Washington Counties, Oregon: Oregon Department of Geology and Mineral Industries Interpretive Map Series IMS–1, 1:62,500.

Madin, I.P., and Mabey, M.A., 1996, Earthquake hazard maps for Oregon: Oregon Department of Geology and Mineral Industries Geological Map Series GMS–100.

Madin, I.P., Priest, G.R., Mabey, M.A., Malone, S., Yelin, T. S., and Meier, D., 1993, March 25, 1993, Scotts Mills

earthquake—western Oregon's wake-up call: Oregon Geology, v. 55, no. 3, p. 51–57.

National Research Council, Commission on Engineering and Technical Systems, Committee on Earthquake Engineering, 1985, Liquefaction of soils during earthquakes: Washington, D.C., National Academy Press, 240 p.

O'Connor, J.E., Sarna-Wojcicki, A., Wozniak, K.C., Polette, D.J., and Fleck, R.J., in press, Origin, extent, and thickness of Quaternary geologic units in the Willamette Valley, Oregon: U.S. Geological Survey Professional Paper 1620.

Priest, G.R., 1995, Explanation of mapping methods and use of the tsunami hazard maps of the Oregon coast: Oregon Department of Geology and Mineral Industries Open-File Report O–95–67, 95 p.

Priest, G.R., and Baptista, A.M., 1995, Tsunami hazard maps of coastal quadrangles, Oregon: Oregon Department of Geology and Mineral Industries Open-File Report O–95–09 through O–95–66 (amended 1997 by O–97–31 and O–97–32), 56 quadrangle maps (as amended).

Ramp, L., and Peterson, N.V., 1979, Geology and mineral resources of Josephine County, Oregon: Oregon Department of Geology and Mineral Industries Bulletin 100, 45 p., 3 geologic maps.

Schlicker, H.G., Deacon, R.J., Beaulieu, J.D., and Olcott, G. W., 1972, Environmental geology of the coastal region of Tillamook and Clatsop Counties; Oregon Department of Geology and Mineral Industries Bulletin 74, 164 p., 18 pls.

Schlicker, H.G., Deacon, R.J., Newcomb, R.C., and Jackson, R.L., 1974, Environmental geology of coastal Lane County, Oregon: Oregon Department of Geology and Mineral Industries Bulletin 85, 116 p., 3 maps.

Seed, H.B., and Idriss, I.M., 1982, Ground motions and soil liquefaction during earthquakes: Earthquake Engineering Institute Monograph, 134 p.

Snavely, P.D., Jr., MacLeod, N.S., Wagner, H.C., and Rau, W.W., 1976, Geologic map of the Cape Foulweather and Euchre Mountain quadrangles, Lincoln County, Oregon: U.S. Geological Survey Miscellaneous Investigations Series Map I–868, 1:62,500.

Ticknor, R., 1993, Late Quaternary crustal deformation on the central Oregon coast as deduced from uplifted wave-cut platforms: Bellingham, Wash., Western Washington University master's thesis, 70 p.

Trimble, D.E., 1963, Geology of Portland, Oregon, and adjacent areas: U.S. Geological Survey Bulletin 1119, 119 p.

Waitt, R.B., 1985, Case for periodic, colossal jökulhlaups from Pleistocene glacial Lake Missoula: Geological Society of America Bulletin, v. 96, no. 10, p. 1271–1286.

Walker, G.W., and McLeod, N.S., 1991, Geologic map of Oregon: U.S. Geological Survey Special Geologic Map, 1:500,000.

Wang, Y., Keefer, D.K., and Wang, Z., 1998, Seismic hazard mapping in Eugene-Springfield, Oregon: Oregon Geology, v. 60, no. 2, p. 31–41.

Wang, Y., and Leonard, W.J., 1996, Relative earthquake hazard maps of the Salem East and Salem West quadrangles, Marion and Polk Counties, Oregon: Oregon Department of Geology and Mineral Industries Geological Map Series GMS–105, 1:24,000.

Wang, Y., and Priest, G.R., 1995, Relative earthquake hazard maps of the Siletz Bay area, coastal Lincoln County, Oregon: Oregon Department of Geology and Mineral Industries Geological Map Series GMS–93, 1:12,000 and 1:24,000.

Wang, Z., Wang, Y., and Keefer, D.K., 1999, Earthquake-induced rockfall and slide hazard along U.S. Highway 97 and Oregon Highway 140 near Klamath Falls, Oregon, *in* Elliott, W.M., and McDonough, P., eds., Optimizing post-earthquake lifeline system reliability. Proceedings of the 5th U.S. Conference on Lifeline Earthquake Engineering, Seattle, Wash., August 12–14, 1999: Reston, Va., American Society of Civil Engineers, Technical Council on Lifeline Earthquake Engineering Monograph 16, p. 61–70.

Weaver, C.S., and Shedlock, K.M., 1989, Potential subduction, probable intraplate, and known crustal earthquake source areas in the Cascadia subduction zone, *in* Hayes, W.W., ed., Third annual workshop on earthquake hazards in the Puget Sound/Portland area, proceedings of Conference XLVIII: U.S. Geological Survey Open-File Report 89–465, p. 11–26.

Wiley, T.J., Sherrod, D.R., Keefer, D.K., Qamar, A., Schuster, R.L., Dewey, J.W., Mabey, M.A., Black, G.L., and Wells, R.E., 1993, Klamath Falls earthquakes, September 20, 1993—including the strongest quake ever measured in Oregon: Oregon Geology, v. 55, no. 6, p. 127–134.

Wilkinson, W.D., Lowry, W.D., and Baldwin, E.M., 1946, Geology of the St. Helens quadrangle, Oregon: Oregon Department of Geology and Mineral Industries Bulletin 31, 39 p., 1 map, 1:62,500.

Yamaguchi, D.K., Atwater, B.F., Bunker, D.E., Benson, B.E., and Reid, M.S., 1997, Tree-ring dating the 1700 Cascadia earthquake: Nature, v. 389, p. 922.

Yeats, R.S., Graven, E.P., Werner, K.S., Goldfinger, C., and Popowski, T., 1991, Tectonics of the Willamette Valley, Oregon: U.S. Geological Survey Open-File Report 91–441–P, 47 p.

Yelin, T.S., Tarr, A.C., Michael, J.A., and Weaver, C.S., 1994, Washington and Oregon earthquake history and hazards: U.S. Geological Survey Open-File Report 94–226–B, 11 p.

APPENDIX

1. Geologic Units Used in Table A-1

Qaf Fine-grained Quaternary alluvium; river and stream deposits of sand, silt, and clay

Qac Coarse-grained Quaternary alluvium; river and stream deposits of sand and gravel

Qmf Fine-grained Quaternary Missoula flood deposits; sand and silt left by catastrophic glacial floods

Qmc Coarse-grained Quaternary Missoula flood deposits; sand and gravel left by catastrophic glacial floods

Qmf1 Fine-grained Quaternary Missoula flood deposits; upper, oxidized low-velocity layer

Qmf2 Fine-grained Quaternary Missoula flood deposits; lower, reduced high-velocity layer

Qe Quaternary estuarine sediments; silt, sand, and mud deposited in bays and tidewater reaches of major rivers

Qs Quaternary sands; beach and dune deposits along the coast

Qmt Quaternary marine terrace deposits; sand and silt deposited during previous interglacial periods

QPe Pleistocene estuarine sediments; older sand and mud deposited in bays and tidewater reaches of rivers

QTac Older coarse-grained alluvium; sand and gravel deposited by ancient rivers and streams

QTaf Older fine-grained alluvium; sand and silt deposited by ancient rivers and streams

Grus Decomposed granite

Tbs Sedimentary bedrock

Tbv Volcanic bedrock

KJg Granite bedrock

KJm Metamorphic bedrock

2. TABLE A-1, MEASURED SHEAR WAVE VELOCITIES[1]

URBAN AREA	SITE #	LAT	LONG	T-1	V-1	U-1	T-2	V-2	U-2	T-3	V-3	U-3	T-4	V-4	U-4
						IMS–7									
Dallas	Dalla01	44.9287	-123.3222	3.4	165	Qmf	0.0	755	Tbs	—	—	—	—	—	—
Dallas	Dalla02	44.9218	-123.3001	2.7	174	Qmf	0.0	780	Tbs	—	—	—	—	—	—
Hood River	Hoodr01	45.7057	-121.5268	4.5	145	Qaf	0.0	1352	Tbv	—	—	—	—	—	—
Hood River	Hoodr02	45.6893	-121.5190	1.0	139	n.d.	6.0	271	QTac	38.0	377	QTac	0.0	995	Tbv
McMinnville-	McMin01	45.2052	-123.2321	5.8	180	Qmf1	0.0	1371	Tbv	—	—	—	—	—	—
McMinnville-	McMin02	45.2112	-123.1383	7.0	201	Qmf1	0.0	277	Qmf2	—	—	—	—	—	—
McMinnville-	McMin03	45.2290	-123.0655	5.6	213	Qmf1	31.7	241	Qmf2	25.3	460	QTaf	0.0	914	Tbs
Monmouth-	Monm01	44.8649	-123.2181	2.3	169	Qmf	15.0	325	Qac	29.1	550	QTaf	0.0	1138	Tbv
Monmouth-	Monm02	44.8425	-123.2027	7.0	159	Qmf	21.1	275	QTac	0.0	403	QTaf	—	—	—
Newberg-	Newb01	45.3123	-122.9494	4.9	220	Qmf1	0.0	513	Tbs	—	—	—	—	—	—
Newberg-	Newb02	45.2945	-122.9735	7.9	162	Qmf1	0.0	330	QTaf	—	—	—	—	—	—
St. Helens-	STH01	45.8516	-122.8104	1.0	88	Qaf	0.0	1204	Tbv	—	—	—	—	—	—
St. Helens-	STH02	45.8562	-122.8364	1.0	40	n.d.	0.0	830	Qac	—	—	—	—	—	—
St. Helens-	STH03	45.8619	-122.7992	1.5	132	Qaf	0.0	710	Qac	—	—	—	—	—	—
Sandy	Sandy01	45.4029	-122.2745	4.5	286	Tbs	0.0	610	Tbs	—	—	—	—	—	—
Sheridan	Sher01	45.0948	-123.3898	3.4	125	Qmf	0.0	749	Tbs	—	—	—	—	—	—
Willamina	Willa01	45.0769	-123.4811	1.0	124	Qmf	3.0	386	QTaf?	0.0	773	Tbs	—	—	—
						IMS–8									
Canby-Aurora	Canb01	45.2682	-122.6859	2.5	266	Qmf	0.0	680	Qmc	—	—	—	—	—	—
Canby-Aurora	Canb02	45.2550	-122.6979	3.5	160	Qmf	0.0	657	Qmc	—	—	—	—	—	—
Lebanon	Lebanon01	44.5293	-122.9104	3.0	144	Qac	0.0	598	Tbv	—	—	—	—	—	—
Lebanon	Lebanon02	44.5517	-122.8945	4.9	244	QTac	0.0	665	Tbv	—	—	—	—	—	—
Silverton	Silvert01	45.0166	-122.7881	1.0	196	Qmf	3.0	818	QTaf	0.0	1402	Tbv	—	—	—
Mt. Angel	Mtag01	45.0731	-122.7897	3.7	184	Qmf	10.0	438	QTac	0.0	1087	Tbv	—	—	—
Stayton	Stayt01	44.8311	-122.7879	3.0	216	n.d.	0.0	551	Tbv	—	—	—	—	—	—
Stayton	Stayt02	44.8047	-122.8014	1.8	142	Qac	0.0	958	Tbv	—	—	—	—	—	—
Sweet Home	Sweet01	44.3955	-122.7234	6.1	203	Qac	0.0	855	Tbv	—	—	—	—	—	—
Woodburn-	Hub01	45.1871	-122.8026	1.0	101	n.d.	11.2	244	Qmf1	0.0	364	Qmf2	—	—	—
Woodburn-	Wood01	45.1451	-122.8228	6.1	247	Qmf1	33.5	341	Qmf2	0.0	396	QTaf	—	—	—
Woodburn-	Wood02	45.1350	-122.8695	6.7	230	Qmf1	0.0	366	Qmf2	0.0	415	QTaf	—	—	—
Woodburn-	Wood03	45.1538	-122.8499	4.5	211	Qmf1	0.0	303	Qmf2	—	—	—	—	—	—

[1] Measurements are for up to four successive identified layers (1 to 4) numbered from the surface down. T = thickness of layer (m); V = Shear wave veolocity (m / s); U = Identified rock unit; n.d. = not determined. Where measurements did not reach bottom of layer, thickness is given as 0.0.

2. TABLE A-1, MEASURED SHEAR WAVE VELOCITIES, CONTINUED

URBAN AREA	SITE #	LAT	LONG	T-1	V-1	U-1	T-2	V-2	U-2	T-3	V-3	U-3	T-4	V-4	U-4
						IMS–9									
Ashland	Ashl01	42.2084	-122.7127	2.0	194	Qaf	6.2	720	Grus	0.0	1220	Kjg	—	—	—
Ashland	Ashl02	42.1912	-122.6857	8.5	327	Qac	13.5	640	Grus	0.0	1015	Kjg	—	—	—
Cottage Grove	Cottage01	43.7856	-123.0651	3.4	219	Qac	0.0	973	Tbs	—	—	—	—	—	—
Cottage Grove	Cottage02	43.7968	-123.0331	3.6	187	Qac	0.0	1270	Tbs	—	—	—	—	—	—
Grants Pass	Grantp01	42.4578	-123.3286	2.4	257	Qac	0.0	506	Grus?	—	—	—	—	—	—
Grants Pass	Grantp02	42.4458	-123.3135	1.5	134	Qaf	7.0	371	Qac	0.0	925	Grus	—	—	—
Grants Pass	Grantp03	42.4244	-123.3449	0.6	321	n.d.	2.1	554	Qac	0.0	868	Grus	—	—	—
Roseburg	Roseb01	43.2159	-123.3668	6.0	181	Qac	0.0	944	Tbv	—	—	—	—	—	—
Sutherlin	Sutherl01	43.3822	-123.3306	5.0	426	Qaf	0.0	842	Tbs	—	—	—	—	—	—
Oakland	Oakland1	43.4221	-123.2988	9.1	198	Qaf	0.0	1079	Tbs	—	—	—	—	—	—
						IMS–10									
Astoria	Ast01	46.1889	-123.8169	10.0	181	Qs	0.0	523	Tbs	—	—	—	—	—	—
Astoria	Ast02	46.1553	-123.8254	5.0	70	Qe	0.0	133	Qs	—	—	—	—	—	—
Astoria	Ast03	46.1530	-123.8877	8.2	81	Qe	0.0	151	Qs	—	—	—	—	—	—
Warrenton	War02	46.2049	-123.9516	0.0	190	Qs	—	—	—	—	—	—	—	—	—
Warrenton	War01	46.1724	-123.9209	5.5	95	Qe	0.0	210	Qs	—	—	—	—	—	—
Brookings	Brook01	42.0570	-124.2809	0.0	183	n.d.	6.0	481	Qmt	0.0	1172	Kjm	—	—	—
Coquille	Coquil01	43.1854	-124.1941	9.5	191	Qaf	0.0	385	Tbs	—	—	—	—	—	—
Coquille	Coquil02	43.1759	-124.1981	27.0	151	Qaf	0.0	589	Tbs	—	—	—	—	—	—
Florence-Dunes City	Floren01	43.9920	-124.1062	11.2	218	Qs	0.0	313	Qs	—	—	—	—	—	—
Florence-Dunes City	Floren02	43.9714	-124.1008	4.4	241	Qs	0.0	371	Qs	—	—	—	—	—	—
Florence-Dunes City	DuneC01	43.9266	-124.0989	4.0	174	Qs	0.0	576	Tbs	—	—	—	—	—	—
Lincoln City	Lincoln01	44.9805	-124.0020	4.3	185	Qmt	0.0	958	Tbs	—	—	—	—	—	—
Lincoln City	Lincoln02	44.9305	-124.0121	0.0	282	Qs	—	—	—	—	—	—	—	—	—
Lincoln City	Lnp01	44.9142	-124.0179	8.0	225	Qs	—	—	—	—	—	—	—	—	—
Newport	Newp01	44.6399	-124.0504	1.0	200	Qs	6.7	448	Qmt	0.0	613	Tbs	0.0	0	
Newport	Newp02	44.6156	-124.0608	17.0	324	Qs	0.0	419	Qmt	—	—	—	—	—	—
Reedsport-Winchester Bay	Reedp01	43.7179	-124.0914	6.4	89	Qe	8.5	144	QPe	0.0	262	QPe	0.0	0	
Reedsport-Winchester Bay	Reedp02	43.6919	-124.1220	3.9	142	QPe	0.0	749	Tbs	—	—	—	—	—	—
Seaside-Cannon Beach	Seas01	45.9786	-123.9289	6.7	274	Qs	0.0	365	Qs	—	—	—	—	—	—
Seaside-Cannon Beach	Seas02	46.0093	-123.9144	12.2	170	Qs	0.0	262	Qs	—	—	—	—	—	—
Seaside-Cannon Beach	Seas03	46.0302	-123.9196	15.5	208	Qs	0.0	280	Qs	—	—	—	—	—	—
Tillamook	Tillam01	45.4629	-123.7993	2.4	335	QTac	0.0	610	Tbs	—	—	—	—	—	—
Tillamook	Tillam02	45.4356	-123.8423	17.0	82	Qe	0.0	308	QTac	—	—	—	—	—	—
Tillamook	Tillam03	45.4712	-123.8503	17.4	83	Qe	0.0	250	QTac	—	—	—	—	—	—

3. COLLECTION AND USE OF SHEAR-WAVE VELOCITY DATA

This section describes our technique for collecting and applying the shear-wave velocity data shown in the preceding table (Table A-1). The table is also available on the accompanying CD-ROM disk as a Microsoft Excel™ spreadsheet.

SH-wave data were collected by means of a 12-channel Bison 5000 seismograph with 8-bit instantaneous floating point and 2048 samples per channel. The data were recorded at a sampling rate between 0.025 and 0.5 ms, depending upon site conditions. The energy source for SH-wave generation is a 1.5 m section of steel I-beam struck horizontally by a 4.5-kg sledgehammer. The geophones used for recording SH-wave data were 30-Hz horizontal component Mark Product geophones. Spacing between the geophones is 3.05 m (10 ft). We used the walkaway method (Hunter and others, 1984), in which a group of 12 in-line geophones remained fixed and the energy source was "stepped out" through a set of predefined offsets. Depending upon site-geological conditions, the offsets of 3.05 m (10 ft), 30.5 m (100 ft), 61.0 m (200 ft), 91.5 m (300 ft), 122 m (400 ft), and 152.4 m (500 ft) were used. In order to enhance the SH-wave and reduce other phases, 5-20 hammer strikes on each site of the steel I-beam were stacked and recorded for each offset.

The SH-wave data were processed on a PC computer using the commercial software SIP by Rimrock Geophysics, Inc. (version 4.1, 1995). The key step for data processing is to identify the refractions from different horizons. Figure A-1 shows the composited SH-wave refraction profile generated from the individual offset records, at site McMin03 (Table A-1) near Dayton, Oregon. Four refractions, R1, R2, R3, and R4 are identified in the profile.

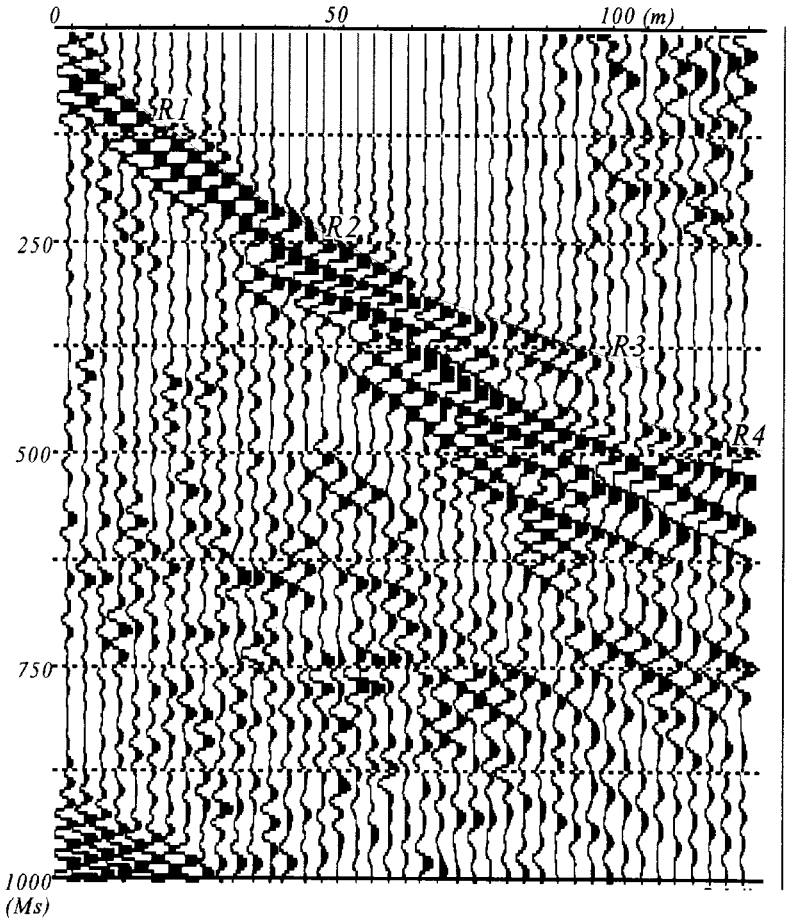

Figure A-1. Composited SH-wave refraction profile at site McMin03.

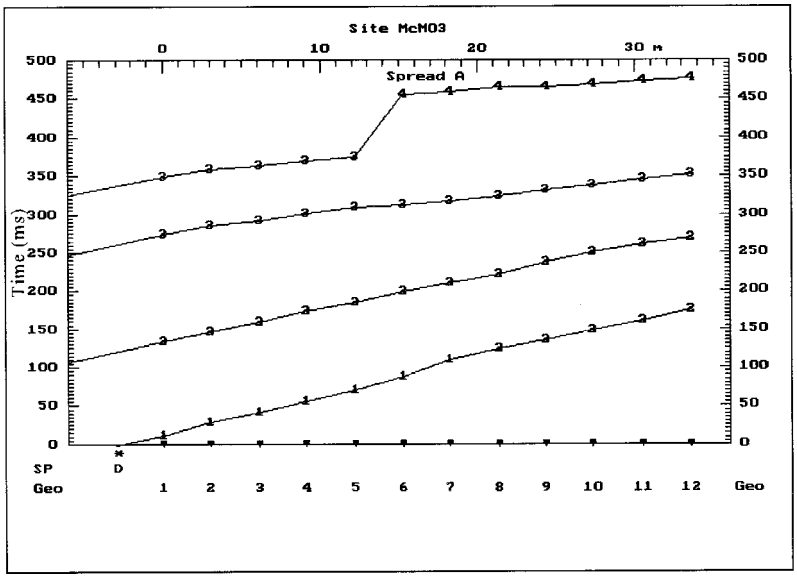

Figure A-2. Arrival time curves of the refractions at site McMin03.

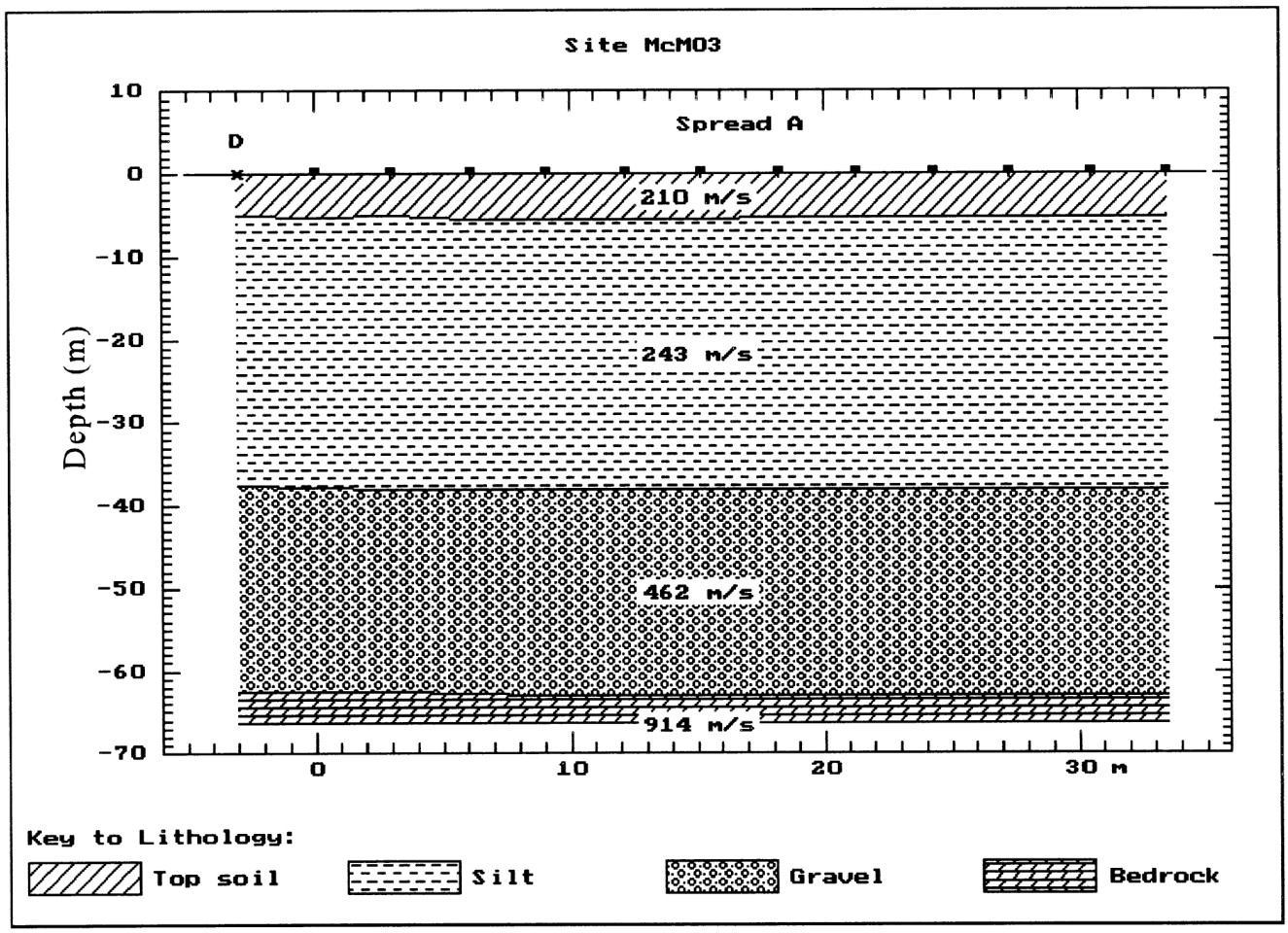

Figure A-3. Shear-wave velocity model interpreted from refraction data at site McMin03.

Arrival times of the refractions were picked interactively on the PC using the BSIPIK module in SIP. The arrival time data picked from each offset record were edited and combined in the SIPIN module to generate a data file for velocity-model deduction.

Figure A-2 shows the arrival times for the refractions identified in the profile (Figure A-1). The shear-wave velocity model is generated automatically using the SIPT2 module. Figure A-3 shows the shear-wave velocity model derived from the refraction data at site McMin03 (Figure A-1). The model is used to calculate an average shear-wave velocity.

The average shear-wave velocity (νs) over the upper 30 m of the soil profile is calculated with the formula of the Uniform Building Code (International Conference of Building Officials, 1997):

$$\nu_s = 30m/\Sigma\{d_i/\nu_{si}\}$$

Where: d_i = thickness of layer i in meters and
v_{si} = shear-wave velocity of layer i in m / s.

Based on the average shear-wave velocity and the UBC-97 soil profile categories as shown in Table 1 above (page 4), the UBC-97 soil classification map is generated with MapInfo® and Vertical Mapper®. Soil types S_E and S_F can not be differentiated from the average shear-wave velocity. S_E and S_F are differentiated based on geologic and geotechnical data, and engineering judgement.